Elastic moduli of porous polymeric biomaterials using 3D microCT image and FE characterization

Jing Jing, Rachid Rahouadj, J. Braux, Frédéric Velard, Dominique Laurent-Maquin, Larbi Siad, Jean-François Ganghoffer, Sophie Gangloff, Halima Kerdjoudj

Elastic moduli of porous polymeric biomaterials using 3D μCT image stack and FE characterization

J. JING[a], R. RAHOUADJ[b], L. SIAD[a], J. BRAUX[a], F. VELARD[a], J.-F. SCHMITT[b], D. LAURENT-MAQUIN[a], J.-F. GANGHOFFER[b] , S.C. GANGLOFF[a], H. KERDJOUDJ[a]

a. BIOS EA 4691, Université de Reims, 51100 Reims, {a}@univ-reims.fr
b. LEMTA UMR , Université de Lorraine, 54504 Vandœuvre-lès-Nancy, {b}@univ-lorraine.fr

Résumé :

Cette étude expérimentale et numérique vise à proposer une procédure permettant l'obtention rapide d'une estimation des modules d'élasticité des phases solides de biomatériaux poreux à base de polymères naturels destinés à l'ingénierie tissulaire de l'os. La procédure s'appuie sur la comparaison des résultats expérimentaux fournis par des essais de compression simple réalisés sur trois éprouvettes cylindriques et des résultats de calculs aux éléments finis de divers éléments parallélépipèdiques réputés être représentatifs du matériau considéré. Ces derniers sont de tailles différentes et arbitrairement répartis au sein de deux reconstructions à très haute résolution par tomographie à rayons X des éprouvettes testés. Pour cette première étude, le matériau constitutif de la phase solide est supposé élastique linéaire, par souci de simplification.

Abstract :

*The objective of this experimental and computational study was to propose a rapid procedure allowing the obtention of an estimation of elastic moduli of solid phases of porous natural-polymeric biomaterials used for bone tissue engineering. This procedure was based on the comparison of experimental results to finite element (FE) responses of parallelepiped so-called representative volume elements (**rev**) of the material at hand. To address this issue a series of quasi-static unconfined compression tests were designed and performed on three prepared cylindrical biopolymer samples. Subsequently, a computed tomography scan was performed on fabricated specimens and two 3D images were reconstructed. Various parallelepiped **rev**s of different sizes and located at distinct places within both constructs were isolated and then analyzed under unconfined compressive loads using FE modeling. In this preliminary study, for the sake of simplicity, the solid phase constituent is assumed to be linear elastic.*

Mots clefs : Biomatériaux poreux. Éléments finis. microtomographie. Élasticité.

1 Introduction

Polysaccharides have emerged as promising biomaterials for tissue engineering purposes. By way of example, among these biological polymers, the naturally abundant and renewable polymers, namely chitosan (CHI) and hyaluronic acid (HA), have excellent properties such as, biocompatiblity, biodegradability, and absorption [5, 10]. On the other hand, considerable attention has been focused on microcomputed tomography (μCT), a non-destructive technique, which yields 3D information of the material analyzed through high-fidelity models constructed from data images. Besides, nowadays image-based meshing offers interesting opportunities based on microstructures scan data to computational continuum micromechanics methods for material characterization [2]. This approach turns out to be very attractive in materials science where the link between macroscopic properties and the micro-structure of a material is sought [6].

2 Materials and methods

2.1 Specimen preparation

Firstly, 2% (w/v) of chitosan was neutralized by the addition of β-glycerol-phosphate (β-GP). Secondly, 0.6% (v/v) of hyaluronic acid was drop-added with a volume ratio of 3:1. Hydrogels were obtained by chemical crosslinking through the addition of genipin at 37 °C for about twelve hours. Finally, 3D porous scaffolds were manufactured according the freeze-drying procedure. The porosity of the investigated cylindrical samples, measured by the liquid displacement method, was estimated to range from 80 to 91% with a pore size of 50 to 150 μm, Fig. 1.

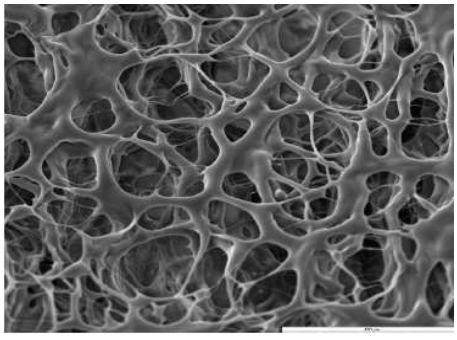

(a) Crosslinked scaffold; scale bar: 100 μm.

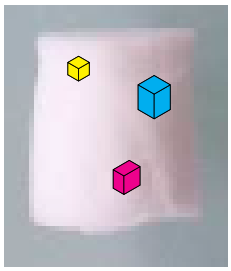

(b) Sample for uniaxial compression test.

Figure 1: (a) SEM image of crosslinked scaffold. (b) Circular cylindrical specimens for unconfined compression test and various so-called representative volume elements of different sizes and located at distinct places.

2.2 Unconfined compression tests

As a porous material, chitosan-hyaluronic acid based biomaterial tend to involve compressive loading. The unconfined (or uniaxial) compression test is often chosen to characterize porous materials because of the simplicity of the testing configuration and the specimen test shape. A typical compression test involves influence of specimen size, influence of porosity, and strain rates effects on mechanical response of the material. Usually compression data including *e.g.*, Young's modulus, yield stress and Poisson's ratio, is obtained from the measured force versus displacement curve. In this preliminary work, unconfined compression tests were carried out first in order to obtain an appraisal of the Young's modulus E of built scaffolds.

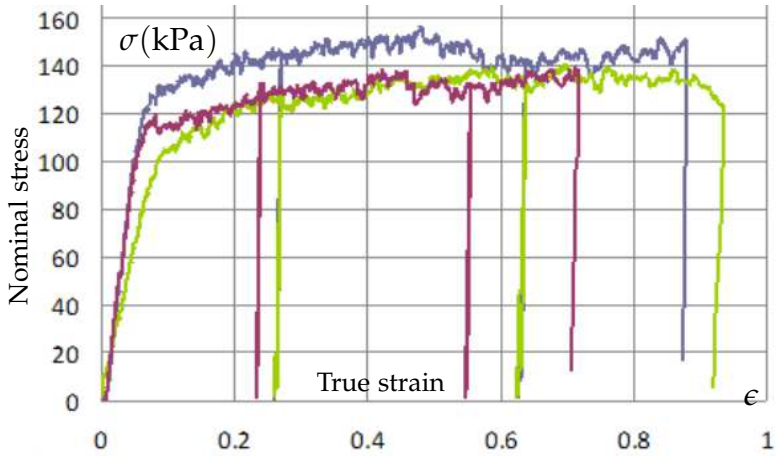

Figure 2: Unconfined compression tests: nominal stress *vs.* true strain curves for crosslinked scaffolds. The 3 curves correspond to 3 distinct samples.

Circular cylindrical samples with about 10.0 mm in diameter and 9.0 mm in height were subject to unconfined compression through an universal testing machine at a strain rate of 2.0×10^{-3} s^{-1}. Both chemical crosslinked and uncrosslinked scaffolds were tested. In this communication the focus only is on the former biomaterial for which Fig. 2 displays the obtained stress-strain curves due to loading (increasing strain) and unloading (decreasing strain) for three distinct samples. The curves seem to be linear for stresses up to about 100 kPa. The mean values of Young' moduli of the samples were measured as the slopes of linear elastic unloading curves. The averaged *apparent* experimental Young's modulus of the crosslinked scaffold was estimated to be equal to 19.20 MPa.

3 Finite element modelling

High-resolution three-dimensional μCT scan data of cylindrical samples were obtained and the data were straightforwardly segmented using threshold and flood fill tools in Simpleware's ScanIP software [9]. The pixel size was 8.85 μm. The 3D connectivity of the hard phase (polymer) turns out to be practically totally interconnected, Fig. 1. As a trade-off, various parallelepiped specimens having the same cross section A_o (0.345×0.345, 0.522×0.522, 0.699×0.699 and $0.965 \times 0.965\,\text{mm}^2$) with increasing thickness h_o (0.345, 0.531, 0.708, and 0.965 mm) were used in this preliminary investigation. They were extracted from the 3D image as shown in Fig. 1 (b). The corresponding 3D μCT image data are converted into FE models. The parallelepiped specimens were meshed with the same mesh density. The anti-aliasing techniques implemented in this software are volume, topology and geometry preserving. Mixed hexahedral and tetrahedral elements were generated. The element parameters were adjusted to the software recommended aspect ratio in order to ensure the highest mesh quality possible [9].

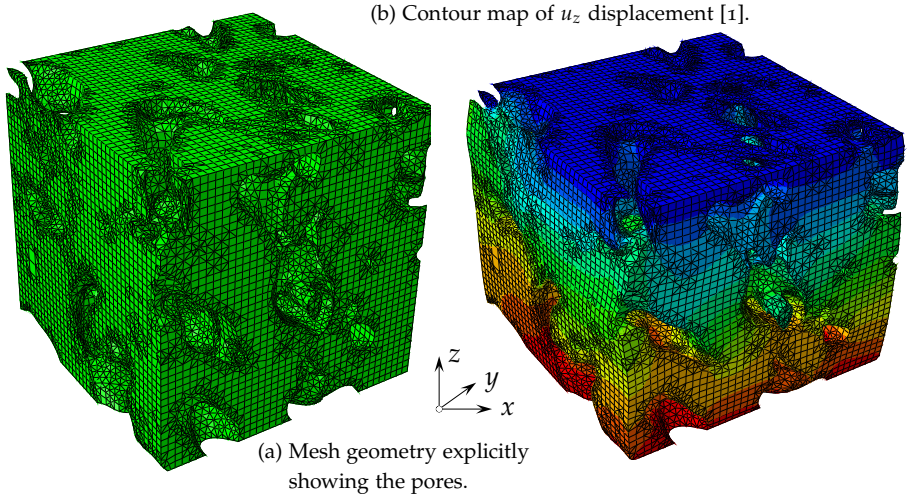

(b) Contour map of u_z displacement [1].

(a) Mesh geometry explicitly showing the pores.

Figure 3: (a) FE mesh of a parallelepiped created from tomographic images [9]. (b) 3D visualization of the contour plot of the displacement component u_z.

The various samples were subject to compression tests along the z-direction. To this goal, a displacement which amplitude depends on the considered sample is imposed on top faces perpendicular to the z-direction, whereas the bottom faces were fixed along z-direction and the four other faces remain free. We made the assumption that the behavior of the solid phase of the considered porous biomaterials remains linear elastic during the whole process of deformation. A series of FE analyses using Abaqus [1] were carried out under compression loading conditions up to approximately 30% strain. It is believed

that this is high enough to observe local deformation. By way of illustration, Fig. 3 (a) shows a typical mesh geometry created from tomographic images using Simpleware [9]. Prior to simulation as such, a wide number of analyses were performed in order to get insight of the sensitivity of numerical predictions to mesh density and segmentation parameters. Force and z-displacement were recorded during the simulated compression test. The nominal compression stress σ was calculated as the ratio of the vertical total reaction force F_z of the top moving face on its initial total area A_o: $\sigma = \frac{F_z}{A_o}$. The true strain ϵ is given by $\epsilon = \ln(\frac{u_z}{h_o})$, where u_z is the vertical displacement of the top moving face and h_o is the initial height of the sample under consideration.

4 Results and future directions

The whole simulated parallelepiped specimens exhibited a similar mechanical trend under compression loading. By way of example, Fig. 3 (b) displays a deformed contour plot of the u_z component of the displacement $\underline{\mathbf{u}}$ calculated using the procedure described above. As regard our first simulation, the used values of Young's modulus and Poisson's ratio of the porous biomaterials at hand were obtained from a literature review dealing with chitosan, *e.g.*, [8, 10]. It emerged that using these values yields a large overestimation of the Young' moduli in comparison to experimental results. In this communication the foregoing FE modeling is used, thanks to the linearity of the problem under consideration, to obtain an estimation of the Young's modulus of the chemical crosslinked biomaterials which preparation is shortly presented in subsection 2.1: $E_{ch} \approx 27.73\,\text{MPa}$. Using this value, the calculated *apparent* Young's modulus E_a of the scaffold are reported in Table 1 which also provides its evolution as a function of the volume size of considered **rve**s.

Table 1: Computed *apparent* Young's modulus E_a as a function of the thickness h_o of the simulated parallelepiped representative material volume.

	$E_{ch} = 27.73\,\text{MPa}$	Averaged experimental Young's modulus: 19.20 MPa									
	μCT construct sample 2							μCT construct sample 1			
$h_o\,(\mu m)$	345.2	345.2	345.2	522.2	522.2	692.2	964.5	345.2	522.2	699.2	964.7
E_a (MPa)	15.42	12.99	13.42	15.91	13.26	14.02	13.76	16.94	17.48	17.81	19.20

One has to notice that when the size of the simulated specimen is smaller than the representative volume element of the material, the properties that can be computed are not necessarily the effective properties but merely *apparent* properties of the investigated volume [4]. Within the context of random

heterogeneous materials, it should be kept in mind that larger computer facilities would be necessary in order to analyze specimens with larger sizes. The computer used throughout the present study is a standard PC.

The foregoing numerical model accounts for the micro architecture of the porous polymeric biomaterials at hand. This prior work highlights that FE models based on an accurate 3D model from μCT data are an essential tool to quantify the effects of pores in complex material systems such as polymeric biomaterials. The ease with which models can be generated would allow us to account for, *e.g.*, the hyperelastic and the viscoelastic behaviour of the materials at hand [3, 7]. These constitutive models can be coupled with FE biomechanical simulations to analyse the behaviour of chitosan-hyaluronic acid based materials used as scaffolds for tissue engineering. These extensions are contemplated as future works.

References

[1] ABAQUS/Standard, SIMULIA, Providence; RI, 2012.

[2] S. K. Boyd. Image-Based Finite Element Analysis. *in:* C. W. Sensen and B. Hallgrímson (eds.), Advanced Imaging in Biology and medecine, Springer-Verlag, 2009, Chap. 14, pp. 3–25.

[3] M. Djabourov, K. Nishinari and E. Schacht. *Physical Gels from Biological and Synthetic Polymers*. Cambridge University Press, 2013.

[4] T. Kanit, S. Forest, I. Galliet, V. Mounoury, and D. Jeulin. Determination of the size of the representative volume element for random composites: statistical and numerical approach. Int. J. Solids Struct, 40, (2003), 3647–3679.

[5] In-Y. Kim, S. J. Seo, H. S. Moon, M.-K. Yoo, In-Y. Park, B.-C. Kim and C. S. Cho. Chitosan and its derivatives for tissue engineering applications. Biotechnology Advances, 26, (2008), 1-21.

[6] E. Maire, and P. J. Withers. Quantitative X-ray tomography. International Materials Reviews, 59, (2014), 1–43.

[7] M. L. Oyen. Mechanical characterisation of hydrogel materials, International Materials Reviews, 59, (2014), 44–58.

[8] B. D. Ratner, A. S. Hoffman, F. J. Schoen, and J. E. Lemons. *Biomaterials Sciences, 3rd Edition*, App. 8: Properties of Soft Materials by M. C. L. Martins. Elsevier Inc., 2013.

[9] Simpleware Ltd., Exeter, UK. `http://www.simpleware.com`, 2014.

[10] S. K. Wang, J. Li, and F. Yao. Application of Chitosan-Based Biomaterials in Tissue Engineering. Chap. 9 *in* K. Yao, J. Li, F. Yao, and Y. Yin (eds.), *Chitosan-based hydrogels. Functions and Applications*. SCRC Press, 2012.